Induced Eddy Currents in Simple Conductive Geometries Due to a Time-Varying Magnetic Field

James R. Nagel

***Abstract*—A complete mathematical formalism is introduced to describe the excitation of electrical eddy currents due to a time-varying magnetic field. The process works by applying a quasistatic approximation to Ampere's law and then segregating the magnetic field into impressed and induced terms. The result is a nonhomogeneous vector Helmholtz equation that can be solved analytically for many practical geometries. Four demonstration cases are then solved under a constant excitation field over all space—an infinite slab in one dimension, a longitudinal cylinder in two dimensions, a transverse cylinder in two dimensions, and a sphere in three dimensions. Numerical simulations are also performed in parallel with analytic computations, all of which verify the accuracy of the derived expressions.**

***Index Terms*—eddy currents, quasistatics, current density**

I. Introduction

THE excitation of electrical eddy currents in metal objects is a well-documented phenomenon with many practical applications. For example, eddy current testing is a form of nondestructive probing that detects the presence of cracks in a metal plate by measuring changes in impedance of a current-carrying coil [1], [2]. Levitation melting is another popular technology that uses eddy currents to repel particles against gravity and avoid contact contamination with a physical container [3], [4]. Eddy current separation is likewise a popular method in the scrap recycling industry for separating nonferrous metal particles from other nonmetallic fluff [5], [6]. One recent variation of that method, called electrodynamic sorting, uses stationary electromagnets to separate nonferrous metal particles from other dissimilar metals [7].

Despite the many uses for eddy current technologies, the basic theory of eddy current physics can vary significantly with context. To illustrate, the problem of nondestructive testing is typically modeled in terms of an impressed current density $\mathbf{J}_s$ that excites a magnetic vector potential $\mathbf{A}$. Following the derivation of [8], an expression of this relationship can be shown to obey the vector-Helmholtz equation,

$$\nabla^2\mathbf{A} - j\omega\mu\sigma\mathbf{A} = -\mu\mathbf{J}_s, \tag{1}$$

where ω is angular frequency, σ is electrical conductivity, and μ is the magnetic permeability. However, for the case of eddy current separation with permanent magnets, there is no current density $\mathbf{J}_s$ to work with. Instead, there is only the relative motion between particles and a magnetic field. By applying the appropriate coordinate transformations, one might instead model the system in terms of a fictitious electric field $\mathbf{E}'$ within the laboratory frame of reference and then derive the corresponding eddy currents accordingly [9]. For the case of levitation melting and electrodynamic sorting, both the particle and the magnetic field are now fixed in space. Likewise, the source distribution $\mathbf{J}_s$ is either not known or simply too complex to offer a tractable solution. Instead, all we may know is the applied magnetic field $\mathbf{B}$ acting on a given system.

At least one treatment of the latter scenario is to let $\mathbf{J}_s = 0$ and then solve (1) under carefully-chosen boundary conditions. Such a formulation has been used, for example, to model a metal sphere excited by a uniform, time-varying magnetic field [10], [11], [12]. Unfortunately, the method only seems to work for the special case of a uniform magnetic field and cannot yet produce results for arbitrarily distributed fields. Other canonical problems, such as the excitation of a longitudinal cylinder, cannot be even solved at all through such methods.

What is needed is a formal mathematical theory that addresses the behavior of induced eddy currents in arbitrary conductive geometries, specifically when stimulated by a time-varying magnetic field. This paper seeks to fill that need by revisiting the fundamental theory of eddy currents and deriving a more comprehensive expression out of Maxwell's equations. Following the introduction, Section II derives the fundamental governing equations for eddy current excitation due to an applied magnetic field. Section III continues by solving a simplified problem in one-dimension to demonstrate the formalism. Sections IV and V then expand on that treatment by solving two special cases of an infinite cylinder. We also introduce an alternative formulation of the eddy current theory that can be desirable for improved mathematical symmetry. Section VI then solves for the induced currents within a uniform sphere. Section VII concludes the paper by discussing the theoretical results and their potential applications.

II. Eddy Current Theory

We begin the discussion with Maxwell's curl equations for linear, isotropic, nonmagnetic media in phasor form. Assuming a phasor convention of $Ae^{j\omega t}$, we let $d/dt = j\omega$. Faraday's law and Ampere's law then state that

$$\nabla \times \mathbf{E} = -j\omega\mathbf{B}\ , \tag{2}$$

$$\nabla \times \mathbf{B} = j\omega\mu_0\epsilon_0\mathbf{E} + \mu_0\mathbf{J}\ , \tag{3}$$

where $\mathbf{B}$ is the magnetic field intensity, $\mathbf{E}$ is the electric field intensity, and $\mathbf{J}$ is the conduction current density. The con-

James R. Nagel (james.nagel@utah.edu) is a research associate with the Department of Metallurgical Engineering at the University of Utah in Salt Lake City, Utah. His PhD in electrical engineering with an emphasis on numerical methods and applied electromagnetics.

stants μ_0 and ϵ_0 then denote the permeability and permittivity of free space.

In the context of eddy currents, we are typically only concerned with very low frequencies of operation. We may therefore employ the *quasi-static approximation*, which simply states that the frequency of excitation ω is very small, but nonzero. The main consequence of this assumption is that the displacement current in Ampere's law becomes negligible, provided that the overall size of the system is much smaller than a single wavelength in free space. As a result, Maxwell's equations reduce to

$$\nabla \times \mathbf{E} = -j\omega\mathbf{B} \ , \tag{4}$$

$$\nabla \times \mathbf{B} = \mu_0\mathbf{J} \ . \tag{5}$$

Next, we shall assume the magnetic field $\mathbf{B}$ is comprised of a linear superposition between two distinct contributions. The idea appears to have been introduced by [13] to model eddy currents within square metallic plates, but we are extending that principle to derive a more general theory. The first contribution is the *impressed* field $\mathbf{B}_i$ and is interpreted as a field that has been arbitrarily imposed onto the system by outside forces. The second is the *induced* field $\mathbf{B}_e$, or simply the *eddy* field, that is created by the presence of moving charges within any conductive materials. The total magnetic field is then written as

$$\mathbf{B} = \mathbf{B}_i + \mathbf{B}_e \ . \tag{6}$$

Because $\mathbf{B}_i$ is generated by external agents beyond the region of interest, we may assume that it has zero curl. It is therefore only $\mathbf{B}_e$ that has a nonzero curl, leading us to write

$$\nabla \times \mathbf{B}_i = 0 \ , \tag{7}$$

$$\nabla \times \mathbf{B}_e = \mu_0\mathbf{J} \ . \tag{8}$$

If we now introduce the point form of Ohm's law, we can relate the conduction current density to the electric field via

$$\mathbf{J} = \sigma\mathbf{E} \ . \tag{9}$$

Ampere's law may now be expressed as

$$\nabla \times \mathbf{B}_e = \mu_0\sigma\mathbf{E} \ . \tag{10}$$

Taking the curl of both sides and substituting from Faraday's law then leads us to

$$\nabla \times \nabla \times \mathbf{B}_e = -j\omega\sigma\mu_0\mathbf{B}_i - j\omega\sigma\mu_0\mathbf{B}_e \ . \tag{11}$$

Next, we recall the vector identity

$$\nabla \times \nabla \times \mathbf{B}_e = -\nabla^2\mathbf{B}_e + \nabla(\nabla \cdot \mathbf{B}_e) \ . \tag{12}$$

From Gauss's law, we know that $\nabla \cdot \mathbf{B}_e = 0$ is always true everywhere. The final result is therefore

$$\nabla^2\mathbf{B}_e + k^2\mathbf{B}_e = -k^2\mathbf{B}_i \ , \tag{13}$$

where $k = \sqrt{-j\omega\sigma\mu_0}$ is the complex wavenumber at low frequency. For simplicity, we may always assume the positive root when evaluating k.

We recognize (13) as a standard vector-Helmholtz equation with nonhomogeneous forcing function. It expresses the causal relationship between an impressed magnetic field $\mathbf{B}_i$ and the resulting eddy fields $\mathbf{B}_e$ generated by electrical currents in conductive particles. Using well-known mathematical methods of classical electromagnetic theory [14], [15], analytic solutions to the Helmholtz equation can now be derived for numerous interesting geometries and shall be demonstrated in the following sections.

Once a solution for $\mathbf{B}_e$ has been found, the induced eddy current density $\mathbf{J}$ quickly follows by applying (8). At this point, there are many other interesting parameters one might wish to compute after the fact, depending on the application. For example, electrodynamic sorting is primarily concerned with the net force acting on a particle in an applied magnetic field [7]. This is easily computed via

$$\mathbf{F} = \int \mathbf{J} \times \mathbf{B} \, dV. \tag{14}$$

Alternatively, many processes involving levitation melting or magnetic levitation might be interested in power dissipation P throughout a particle [11]. A very useful expression toward that end would be

$$P = \int \frac{1}{\sigma} \mathbf{J} \cdot \mathbf{J}^* \, dV. \tag{15}$$

III. A One-Dimensional Slab

The simplest solution to (13) involves a one-dimensional slab of infinite extent along the y- and z-axes. Depicted in Fig. 1(a), the slab is assumed to have a uniform conductivity σ throughout its volume and a thickness 2ℓ along the x-direction. The impressed magnetic field is also assumed to be a constant value everywhere such that $\mathbf{B}_i = B_0\hat{\mathbf{z}}$. Since the excitation field only acts along the $\hat{\mathbf{z}}$-direction, we may likewise express the eddy field as $\mathbf{B}_e = B_e(x)\hat{\mathbf{z}}$. Letting $\partial/\partial y = \partial/\partial z = 0$, the resulting Helmholtz equation inside the slab yields

$$\frac{\partial^2 B_e}{\partial x^2} + k^2 B_e = -k^2 B_0 \quad (|x| \leq \ell) \ . \tag{16}$$

Outside of the slab, we note that the wavenumber $k = 0$, reducing the Helmholtz equation to

$$\frac{\partial^2 B_e}{\partial x^2} = 0 \quad (|x| \geq \ell) \ . \tag{17}$$

Beginning with (16), we have a standard, second-order differential equation with inhomogeneous forcing function. The general solution is therefore given as

$$B_e(x) = C_1 \cos(kx) + C_2 \sin(kx) - B_0 \ , \tag{18}$$

where C_1 and C_2 are constants yet to be determined. Due to the symmetry of the system, we can immediately enforce the condition that $B_e(x) = B_e(-x)$, thereby letting $C_2 = 0$. The next condition is that the total magnetic field $B_e + B_0$ must be continuous at $x = \pm\ell$. If we further impose the condition that the total field remain finite as $x \to \pm\infty$, we find that there is zero eddy field extending beyond the boundaries of the slab. Solving for C_1 then quickly leads to $C_1 = B_0/\cosh(k\ell)$, resulting in the eddy field

$$\mathbf{B}_e(x) = B_0 \left[\frac{\cos(kx)}{\cos(k\ell)} - 1 \right] \hat{\mathbf{z}} \quad (|x| \leq \ell) \ . \tag{19}$$

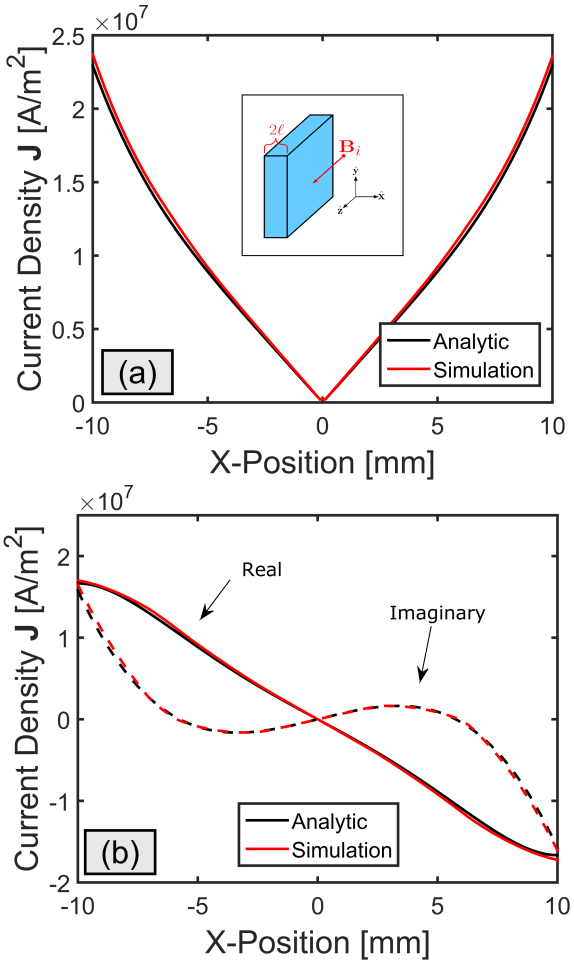

Fig. 1. (a) Current density magnitude $|J_y(x)|$ along a thin metal slab with $2\ell = 20$ mm and $\sigma = 1.0$ MS/m. (b) Real and imaginary components of $J_y(x)$.

To calculate the current density field $\mathbf{J}$, we simply apply (8) to (19) and find

$$\mathbf{J}(x) = \frac{kB_0}{\mu_0}\frac{\sin(kx)}{\cos(k\ell)}\,\hat{\mathbf{y}} \quad (|x| \le \ell)\ . \tag{20}$$

Figures 1(a) and 1(b) show the solutions for J_y computed inside a metal slab with length $\ell = 10$ mm and a conductivity of $\sigma = 1.0$ MS/m. The slab is excited by a magnetic field intensity of $B_0 = 0.1$ T at a frequency of $f = 10$ kHz, which are representative values of electrodynamic sorting. For comparison, numerical simulations were also performed under similar conditions using the CST EM Studio® software package [16]. However, since numerical simulations in three dimensions cannot extend to infinity, the slab was truncated to large, finite values (200 mm × 200 mm × 20 mm).

Agreement between the simulation results and analytic calculations is very strong, thus validating the reliability of our model. It is interesting to note how the eddy currents monotonically grow in magnitude away from the center of the slab, just as one would expect from the greater capture of magnetic flux throughout the cross-sectional area. The phase, however, is not a constant value throughout the slab, but actually varies quite significantly. It is tempting to interpret this as a potential violation of Lenz' law, in that the eddy field is not always directly opposing the changes in applied field $\mathbf{B}_i$. The reality is that the eddy currents are opposing all changes in the *total* magnetic field, meaning that we must also account for the eddy field $\mathbf{B}_e$ at every point along the slab. The result is a highly complicated phase relationship throughout the slab, which is all captured by the analytic expression in (20).

Another point of interest is the fact that the eddy field beyond the boundaries of the slab is identically zero. This is a natural result of the symmetry of the system, wherein any field contribution from some arbitrary current density element within the slab is perfectly canceled out by an equal, opposite contribution on the other end. It is only within the slab that any asymmetry exists and thus realizes a nonzero value for $\mathbf{B}_e$.

Finally, it is instructive to rewrite the current density in terms of complex exponentials such that

$$\mathbf{J}(x) = -\frac{jkB_0}{\mu_0}\frac{e^{jkx} - e^{-jkx}}{e^{jk\ell} + e^{-jk\ell}}\,\hat{\mathbf{y}} \quad (|x| \le \ell)\ . \tag{21}$$

Notice how this reveals the current density to be superposition of a forward-traveling wave and a reverse-traveling wave. We can further break up the wavenumber into real and imaginary components using $k = q - jq$ with $q = \sqrt{\omega\mu_0\sigma/2}$. Substitution back into the previous expression then gives

$$\mathbf{J}(x) = -\frac{jkB_0}{\mu_0}\frac{e^{qx}e^{jqx} - e^{-qx}e^{-jqx}}{e^{q\ell}e^{jq\ell} + e^{-q\ell}e^{-jq\ell}}\,\hat{\mathbf{y}} \quad (|x| \le \ell)\ . \tag{22}$$

We now see that each wave is associated with a real exponential decay of $e^{\pm qx}$ in the forward and reverse directions. We thus define the decay length $1/q$ as the *skin-depth* δ of the material where

$$\delta = \sqrt{\frac{2}{\omega\mu_0\sigma}}\ , \tag{23}$$

which is consistent with the results of previous works [8], [11].

IV. Longitudinal Excitation of a Cylinder

The next system of interest is a long cylinder with radius a being excited longitudinally down its primary axis. We can express this scenario by orienting the cylinder along the z-axis and then exciting the system with the impressed field $\mathbf{B}_i = B_0\hat{\mathbf{z}}$. Due to the symmetry of the model, it is natural to express the eddy field in cylindrical coordinates such that $\mathbf{B}_e = B_e(\rho)\hat{\mathbf{z}}$ and $\partial/\partial\phi = \partial/\partial z = 0$. Writing out the Helmholtz equation accordingly thus produces

$$\rho^2\frac{\partial^2 B_e}{\partial\rho^2} + \rho\frac{\partial B_e}{\partial\rho} + k^2\rho^2 B_e = -k^2\rho^2 B_0 \quad (\rho \le a)\ , \tag{24}$$

where a is defined as the cylinder radius. Outside of the cylinder, we let $k = 0$ and find

$$\rho^2\frac{\partial^2 B_e}{\partial\rho^2} + \rho\frac{\partial B_e}{\partial\rho} = 0 \quad (\rho > a)\ . \tag{25}$$

Outside of the cylinder, the eddy field is governed by a standard second-order differential equation. The solution is thus well-known to satisfy

$$B_e(\rho) = D_1\ln\rho + D_2 \quad (\rho \ge a)\ . \tag{26}$$

Looking at (24), we immediately recognize Bessel's differential equation in nonhomogeneous form. The solution takes the form of a linear combination between the particular solution B_p and the complementary solution B_c. Using Section III as a guide, we assume that the particular solution satisfies $B_p(\rho) = -B_0$. For the complementary solution, the general expression satisfies

$$B_c(\rho) = C_1 J_0(k\rho) + C_2 Y_0(k\rho) \quad (\rho \leq a) \ , \tag{27}$$

where J_0 and Y_0 denote the Bessel functions of the first and second kind with order zero.

For our first boundary condition, we require that B_e remain bounded as $\rho \to 0$. This immediately forces $C_2 = 0$ since the second Bessel function is known to diverge. We likewise require that B_e remain bounded as $\rho \to \infty$, which forces $D_1 = D_2 = 0$ and thus zero eddy field beyond the cylinder. For our final condition, we require the total magnetic field to be continuous across the boundary at $\rho = a$. Solving for the final coefficient then results in $C_1 = B_0/J_0(ka)$, and the eddy field becomes

$$\mathbf{B}_e(\rho) = B_0 \left[\frac{J_0(k\rho)}{J_0(ka)} - 1 \right] \hat{\mathbf{z}} \quad (\rho \leq a) \ . \tag{28}$$

Substituting (28) into Ampere's law and solving for $\mathbf{J}$, we next arrive at

$$\mathbf{J}(\rho) = -\frac{kB_0}{\mu_0} \frac{J_0'(k\rho)}{J_0(ka)} \hat{\boldsymbol{\phi}} \quad (\rho \leq a) \ . \tag{29}$$

Note the potential confusion in notation between the current density field $\mathbf{J}$ with the Bessel functions J_0 and J_1. For consistency, a numerical subscript shall always refer to a Bessel function whereas an alphabetic subscript shall always refer to a vector component of the current density field. If we finally recall that $J_0'(x) = -J_1(x)$, we can simplify the solution to read

$$\mathbf{J}(\rho) = \frac{kB_0}{\mu_0} \frac{J_1(k\rho)}{J_0(ka)} \hat{\boldsymbol{\phi}} \quad (\rho \leq a) \ . \tag{30}$$

Figure 2(a) shows an example calculation of the eddy current density along the cross-section of a metal cylinder specified by a radius of $a = 10$ mm with a conductivity of $\sigma = 5.0$ MS/m. The excitation field is likewise set to $B_0 = 0.1$ T at a frequency of $f = 10$ kHz. Figure 2(b) shows the real and imaginary components of the J-fields directly down the center of the cylinder. For comparison, a numerical simulation of a very long cylinder (60 mm length) at $z = 0$ is also superimposed on the calculated values.

Just like the infinite slab, we see excellent agreement between the analytic expressions and numerical calculations. As long as the cylinder is very long and the fields are examined far away from the tips, one can reasonably expect (30) to produce an accurate expression of the field profile. It is also interesting to note how the radial flow of current behaves much like an infinite solenoid, which explains why the eddy field outside the cylinder is again identically zero. Furthermore, the skin effect is seen to be much more apparent in this example, due to the increase in conductivity from 1.0 MS/m to 5.0 MS/m. If we recall that the wavenumber satisfies $k^2 = -j\omega\mu_0\sigma$, we can likewise note the linear proportionality between σ and

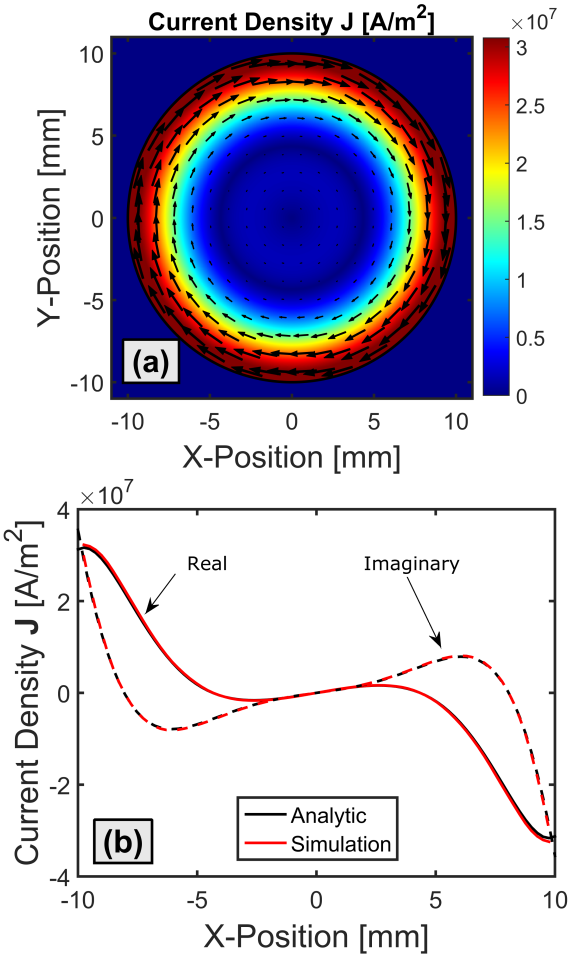

Fig. 2. (a) Current density at time $t = 0$ plotted along a cylindrical cross-section using Equation (30). (b) Real and imaginary components of $J_\phi(x)$ compared to numerical simulation.

ω. That is to say, if the frequency were doubled while the conductivity were reduced by half, then the resulting eddy current field would be perfectly identical.

V. Transverse Excitation of a Cylinder

To complete our evaluation of a conductive cylinder, we now need to consider magnetic excitation along a transverse axis—for example, $\mathbf{B}_i = B_0\hat{\mathbf{x}}$. Any arbitrarily impressed magnetic field can then be expressed as a linear superposition of both a longitudinal component and transverse component with respect to the cylinder. At the same time, however, we immediately encounter a difficult problem in that $\mathbf{B}_i = B_0\hat{\mathbf{x}}$ does not seem to provide any straightforward symmetry by which to solve (13). While it is still technically possible to brute-force a solution through basic numerical methods [17], [18], [19], we would clearly like to devise a workable mathematical framework by which to express an exact solution.

One way to accomplish this goal is to reevaluate (13) in terms of magnetic vector potential. If we recall Gauss' law of $\nabla \cdot \mathbf{B} = 0$, then we can immediately conclude the existence of a separate vector field $\mathbf{A}$ that satisfies

$$\mathbf{B} = \nabla \times \mathbf{A} \ . \tag{31}$$

Substituting into Faraday's law, we quickly find that

$$\nabla \times (\mathbf{E} + j\omega\mathbf{A}) = 0 \ . \tag{32}$$

This expression further implies the existence of a scalar field ϕ that satisfies

$$\mathbf{E} + j\omega\mathbf{A} = -\nabla\phi \ . \tag{33}$$

Plugging (31) into Ampere's law, we find

$$-\nabla^2\mathbf{A} + \nabla(\nabla \cdot \mathbf{A}) = \mu_0\mathbf{J} \ . \tag{34}$$

Applying Ohm's law and (33) next reveals

$$\nabla^2\mathbf{A} + k^2\mathbf{A} = \nabla(\nabla \cdot \mathbf{A} + \mu_0\sigma\phi) \ . \tag{35}$$

As a final step, we observe that the vector potential $\mathbf{A}$ has only been defined in terms of its curl and is thus not yet unique. In order to uniquely specify $\mathbf{A}$, we still need to impose a solution for its divergence. This choice of divergence is called a *gauge*, with the natural choice being $\nabla \cdot \mathbf{A} = -\mu_0\sigma\phi$. The result is a familiar expression with the form of

$$\nabla^2\mathbf{A} + k^2\mathbf{A} = 0 \ . \tag{36}$$

The value of (36) is that it again expresses the physical behavior of eddy currents through a vector Helmholtz equation. The vector potential $\mathbf{A}$, however, is perfectly orthogonal to $\mathbf{B}$, thus opening up new opportunities for a separable expression in cylindrical coordinates. The trade-off, however, is that (36) also gives up the nonhomogeneous source term that served as the forcing function in (13). Fortunately, we can still express the same information via an appropriate choice of boundary conditions. Such a concept has already been used to great advantage by Peter Rony for the case of a uniform sphere [10], and we shall likewise apply the same principle on a transverse cylinder.

We begin by noting that the vector function,

$$\mathbf{A}_i(\rho,\phi) = B_0\rho\sin(\phi)\,\hat{\mathbf{z}} \ , \tag{37}$$

corresponds to the excitation field $\mathbf{B}_i = B_0\hat{\mathbf{x}}$ in cylindrical coordinates[1]. One can immediately verify this fact by calculating $\mathbf{B}_i = \nabla \times \mathbf{A}_i$ and observing the result. We also see that $\mathbf{A}$ is only excited along the $\hat{\mathbf{z}}$-direction, which means that the resulting Helmholtz equation need only be expressed along this same component. The functional form of our solution can therefore be expressed as $\mathbf{A} = A(\rho,\phi)\,\hat{\mathbf{z}}$ with the corresponding Helmholtz equation satisfying

$$\rho^2\frac{\partial^2 A}{\partial\rho^2} + \rho\frac{\partial A}{\partial\rho} + k^2\rho^2 A = -\frac{\partial^2 A}{\partial\phi^2} \ . \tag{38}$$

The solution to (38) is found by applying the method of separation of variables and follows a well-known process found in many standard references [14], [15]. The complete solution for A, both inside and outside of the cylinder, is thus given as

$$A(\rho,\phi) = \big[C_1\cos(\lambda\phi) + C_2\sin(\lambda\phi)\big] \begin{cases} D_1 J_\lambda(k\rho) + D_2 Y_\lambda(k\rho) & (\rho \le a) \\ D_3\rho^{+\lambda} + D_4\rho^{-\lambda} & (\rho > a) \end{cases} \ . \tag{39}$$

[1]Note that ϕ in this context now refers to the azimuth angle of cylindrical coordinates; not the scalar field defined by (33)

For our first boundary condition, we require that A remain finite as $\rho \to 0$ and immediately find that $D_2 = 0$. For our second boundary condition, we require that the fields at infinity must approach the impressed field defined by (37). That is to say,

$$\lim_{\rho\to\infty} A(\rho,\phi) = B_0\rho\sin(\phi) \ . \tag{40}$$

The immediate consequence of this condition is that $\lambda = 1$, $C_1 = 0$, and $D_3 = B_0$. The complete solution for A thus dramatically simplifies to

$$A(\rho,\phi) = \sin(\phi)\begin{cases} D_1 J_1(k\rho) & (\rho \le a) \\ B_0\rho + D_4\rho^{-1} & (\rho > a) \end{cases} \ . \tag{41}$$

At this point, there are only two unknown coefficients, D_1 and D_4. We also note that the eddy fields outside of the cylinder are no longer trivial and thus require more careful consideration. We therefore begin by imposing continuity along the boundary at $\rho = a$, or $A(a^-,\phi) = A(a^+,\phi)$, which leads us to

$$D_1 a J_1(ka) - D_4 = B_0 a^2 \ . \tag{42}$$

The final boundary condition stems from Maxwell's equations and requires that the tangential H-field must remain continuous along the boundary at $\rho = a$, where $\mathbf{H}$ is related to $\mathbf{B}$ via the constitutive relation $\mathbf{B} = \mu\mathbf{H}$. However, since we are only concerned with nonmagnetic materials, we can simplify this condition to require that only the tangential B-field be continuous. That is to say,

$$\hat{\boldsymbol{\rho}} \times \nabla \times \mathbf{A}\Big|_{\rho=a^-} = \hat{\boldsymbol{\rho}} \times \nabla \times \mathbf{A}\Big|_{\rho=a^+} \ . \tag{43}$$

Carrying out this calculation eventually leads to

$$D_1 k a^2 J_1'(ka) + D_4 = B_0 a^2 \ . \tag{44}$$

Taken together, (42) and (44) form a system of equations that uniquely determine D_1 and D_4. Solving this system leads us to the solution

$$D_1 = \frac{2B_0 a}{kaJ_1'(ka) + J_1(ka)} \ , \quad \text{and} \tag{45}$$

$$D_4 = \frac{2B_0 a^2 J_1(ka)}{kaJ_1'(ka) + J_1(ka)} - B_0 a^2 \ . \tag{46}$$

Recalling our gauge condition $\nabla \cdot \mathbf{A} = -\mu_0\sigma\phi$, we notice that the divergence of Equation (41) is zero. As a result, ϕ is also zero and the current density satisfies the very simple relation $\mathbf{J} = -j\omega\sigma\mathbf{A}$. Solving for the total eddy current density finishes with

$$\mathbf{J}(\rho,\phi) = \hat{\mathbf{z}}\left[\frac{-2j\omega\sigma B_0 a}{kaJ_1'(ka) + J_1(ka)}\right] J_1(k\rho)\sin(\phi) \qquad (r \le a) \ . \tag{47}$$

Figures 3(a) and 3(b) show the solution to (47) for a cylinder of radius $a = 10$ mm and conductivity $\sigma = 5.0$ MS/m. The excitation field is given as $B_0 = 0.1$ T at $f = 10$ kHz and is oriented parallel to the x-axis. Simulation results are also plotted down the center of a long (60 mm) cylinder with the same radius a and conductivity σ. As with the transverse case, we can reasonably assume an accurate solution for very long, thin cylinders.

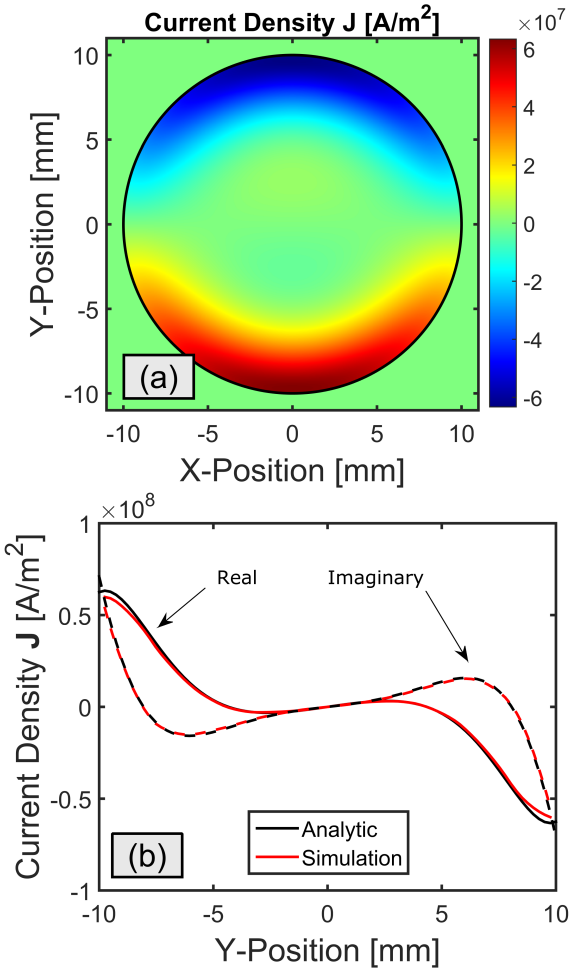

Fig. 3. (a) Current density $J_z(x, y)$ at time $t = 0$ plotted along a cylindrical cross-section using Equation (47). (b) Real and imaginary components of $J_z(0, y)$ compared to numerical simulation.

VI. Excitation of a Sphere

As we found in Section V, the solution for a transverse cylinder can be rather involved. Even so, the process is still relatively straightforward and tractable, eventually giving rise to a compact solution for $\mathbf{J}$. For the special case of a sphere, the overall derivation is generally identical to that of the transverse cylinder except for the use of spherical coordinates rather than cylindrical. As mentioned earlier, the concept was originally introduced by Peter Rony in 1964 [10], but was only used to calculate the net force on a sphere rather than the total eddy current distribution. Bidinosti and others have likewise explored the problem of eddy currents on a sphere [12], but appear to have derived a solution with an incorrect scale factor. What follows here is a simplified reworking of Rony's original derivation, but specifically focused on calculating the eddy current density and verifying the solution against numerical simulations.

Given an impressed magnetic field $\mathbf{B}_i = B_0\hat{\mathbf{z}}$, the equivalent magnetic vector potential in spherical coordinates satisfies

$$\mathbf{A}_i(r, \theta, \phi) = \frac{1}{2} B_0 r \sin(\theta)\, \hat{\boldsymbol{\phi}} \ , \tag{48}$$

where r is the radial coordinate, θ is the elevation angle, and ϕ is the azimuth. One can again verify this expression by computing $\mathbf{B}_i = \nabla \times \mathbf{A}_i$ in spherical coordinates. The field is assumed to excite a spherical particle of radius a and conductivity σ at a frequency $\omega = 2\pi f$. Presuming that the eddy field induced within the sphere decays to zero as $r \to \infty$, (48) can then serve as our boundary condition at infinity.

Noticing that $\mathbf{A}$ is only excited along the $\hat{\boldsymbol{\phi}}$-direction, we let $A_r = A_\theta = 0$. We also note the symmetry around ϕ such that $\partial/\partial\phi = 0$. Expressing Equation (36) in spherical coordinates then leads to

$$\frac{1}{r^2}\frac{\partial}{\partial r}\left(r^2 \frac{\partial A}{\partial r}\right) + \frac{1}{r^2 \sin\theta}\frac{\partial}{\partial \theta}\left(\sin\theta \frac{\partial A}{\partial \theta}\right) - \frac{A}{r^2 \sin^2\theta} + k^2 A = 0 \ , \tag{49}$$

where the scalar function A implicitly denotes $A = A_\phi(r, \theta)$. Assuming separability with the form $A = R(r)\Theta(\theta)$ and recognizing the appropriate differential equations as they arise [20], the complete, general solution for A is expressed as

$$A_\phi(r, \theta) = \left[D_1 P_n^1(\cos\theta) + D_2 Q_n^1(\cos\theta)\right] \begin{cases} C_1\, j_n(kr) + C_2\, y_n(kr) & (r \le a) \\ C_3 r^n + C_4 r^{-n-1} & (r > a) \end{cases} \ . \tag{50}$$

The functions j_n and y_n are the spherical Bessel functions of the first and second kind with order n, whereas P_n^1 and G_n^1 are the associated Legendre functions of the first and second kind.

We are now ready to apply boundary conditions, with the first condition being the requirement for a finite solution at $r = 0$. Since the second Bessel function y_n is divergent, we naturally find $C_2 = 0$. We likewise require that all fields converge to the impressed profile for observers far away from the sphere, thus forcing

$$\lim_{r\to\infty} A_\phi(r, \phi) = \frac{1}{2} B_0 r \sin\theta \ . \tag{51}$$

Noting the identity $P_1^1(\cos\theta) = \sin\theta$, the implied consequence of this condition is that $D_1 = 1$, $D_2 = 0$, $n = 1$, and $C_3 = B_0/2$. Rewriting the solution for A and combining terms thus brings us to the greatly simplified result

$$A_\phi(r, \theta) = \sin\theta \begin{cases} C_1\, j_1(kr) & (r \le a) \\ (1/2) B_0 r + C_4 r^{-2} & (r > a) \end{cases} \ . \tag{52}$$

The coefficients C_1 and C_4 are found by applying continuity of the A-fields and H-fields at $r = a$. The first condition is straightforward and results in

$$C_1\, j_1(ka) = (1/2) B_0 a + C_4 a^{-2} \ . \tag{53}$$

The second condition follows (43) and evaluates to

$$\left.\frac{\partial}{\partial r}(r A_\phi)\right|_{r=a^-} = \left.\frac{\partial}{\partial r}(r A_\phi)\right|_{r=a^+} \ . \tag{54}$$

Calculating the derivatives and substituting for $r = a$ then gives

$$C_1\left[k a j_1'(ka) + j_1(ka)\right] = B_0 a - C_4 a^{-2} \ . \tag{55}$$

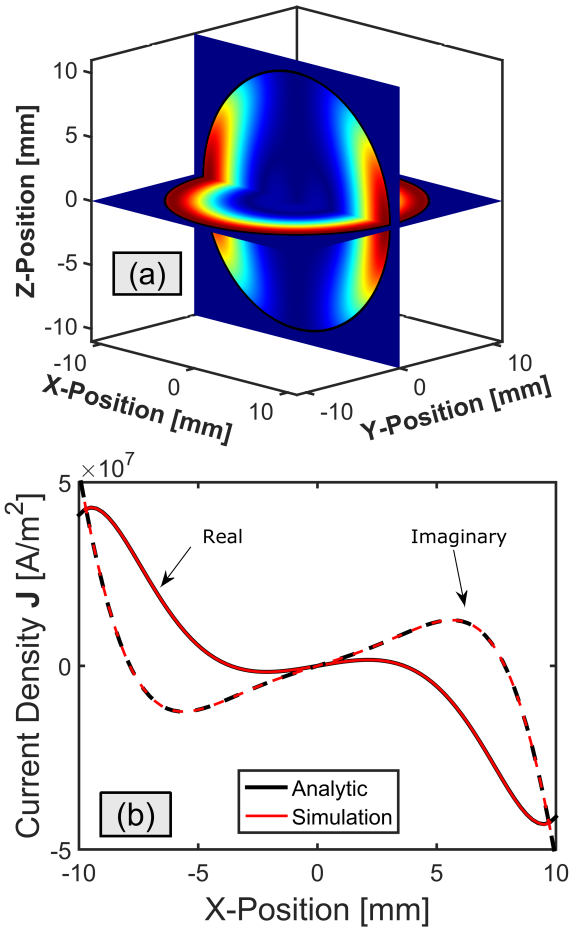

Fig. 4. (a) Current density magnitude $|J_\phi|$ normalized and plotted along two cross-sections of a spherical particle using Equation (58). (b) Real and imaginary components of $J_y(x, 0, 0)$ compared against numerical simulation.

After solving the system of linear equations, we find our last coefficients to be

$$C_1 = \frac{3B_0 a}{2kaj_1'(ka) + 4j_1(ka)} \ , \tag{56}$$

$$C_4 = \frac{B_0 a^3}{2}\left[\frac{6j_1(ka)}{4j_1(ka) + 2kaj_1'(ka)} - 1\right] \ . \tag{57}$$

Noting again that $\nabla \cdot \mathbf{A} = 0$, we can immediately solve for the eddy current density using $\mathbf{J} = -j\omega\sigma\mathbf{A}$. The result is a relatively compact expression with the form

$$\mathbf{J}(r,\theta) = \hat{\boldsymbol{\phi}}\left[\frac{-3j\omega\sigma B_0 a}{2kaj_1'(ka) + 4j_1(ka)}\right] j_1(kr)\sin(\theta) \quad (r \le a) \ . \tag{58}$$

Figure 4(a) shows the solution to Equation (58) for a sphere of radius $a = 10$ mm and conductivity $\sigma = 5.0$ MS/m. The excitation field is given as $B_0 = 0.1$ T at $f = 10$ kHz and is oriented parallel to the z-axis. Figure 4(b) shows the real and imaginary components of J_y when plotted as a function of x at $y = z = 0$. For comparison, simulation results are also plotted against the analytic solution and show excellent agreement.

It is interesting to note how the J-field is mostly concentrated around the equatorial regions of the sphere, with a pronounced skin effect forcing most of the current toward the outer edge. Part of this is due to the $\sin\theta$ dependence, which forces all currents towards zero along the z-axis of the sphere. A similar effect was also seen with the transverse cylinder, which likewise exhibited a $\sin\theta$ dependence. The reason for this is again best explained by a capture of magnetic flux, which increases as one moves away from the center of the sphere towards the outer edge.

VII. Discussion

This work provided a direct mathematical formalism for calculating electrical eddy currents due to the presence of a time-varying magnetic field. Four demonstration cases were solved, including a one-dimensional slab, two orientations of an infinite circular cylinder, and a sphere. For each case, numerical simulations were performed in parallel with the analytic computations and agreed very well with the end result.

While (13) captures the governing behavior of any arbitrary system of interest, it is not necessarily the most straightforward expression to solve under all circumstances. In at least some instances, we have shown that (36) is capable of simplifying the problem into a more tractable derivation. At the same time, however, this is only true for the limited number of cases wherein the appropriate boundary conditions can be expressed at infinity. If, for example, the excitation field were not uniform, then (37) would have to be reinvented and applied accordingly. In contrast, (13) technically describes the eddy current behavior for any arbitrary source field $\mathbf{B}_i$.

Although we have neglected the possibility of magnetic materials in this work, it should be relatively straightforward to produce a similar theory for magnetic metals by simply replacing μ_0 with $\mu_r\mu_0$ in the wavenumber k. When doing so, however, one must be careful to enforce the proper boundary conditions with nonmagnetic media such that all tangential H-fields remain continuous. This means (43) and (54) are only applicable within the scope of this paper and are not generally true expressions. Such issues, however, are best left to follow-up research.

VIII. Acknowledgments

This work was funded by the United States Advanced Research Project Agency-Energy (ARPA-E) METALS Program under cooperative agreement grant DE-AR0000411. The author would also like to thank Professor Raj Rajamani, Jaclyn Ray, and Dawn Sweeney for their insightful edits and proofreading.

References

[1] C. V. Dodd and W. E. Deeds, "Analytical solutions to eddy-current probe-coil problems," *Journal of Applied Physics*, vol. 39, no. 6, pp. 2829–2838, 1968.

[2] J. R. Bowler, "Eddy-current interaction with an ideal crack. 1. the forward problem," *Journal of Applied Physics*, vol. 75, no. 12, pp. 8128–8137, 1994.

[3] E. C. Okress, D. M. Wroughton, G. Comenetz, P. H. Brace, and J. C. R. Kelly, "Electromagnetic levitation of solid and molten metals," *Journal of Applied Physics*, vol. 23, no. 5, pp. 545–552, 1952.

[4] E. Fromm and H. Jehn, "Electromagnetic forces and power absorption in levitation melting," *British Journal of Applied Physics*, vol. 16, no. 5, pp. 653–663, 1965.
[5] F. Maraspin, P. Bevilacqua, and P. Rem, "Modeling the throw of metals and nonmetals in eddy current separations," *International Journal of Mineral Processing*, vol. 73, no. 1, pp. 1–11, 2004.
[6] M. Lungu and P. Rem, "Separation of small nonferrous particles using an inclined drum eddy-current separator with permanent magnets," *IEEE Transactions on Magnetics*, vol. 38, no. 3, pp. 1534–1538, 2002.
[7] N. Dholu, J. R. Nagel, D. Cohrs, and R. K. Rajamani, "Eddy current separation of nonferrous metals using a variable-frequency electromagnet," *KONA Powder and Particle Journal*, pp. 1–7, 2016.
[8] T. P. Theodoulidis and E. E. Kriezis, *Eddy current canonical problems (with applications to nondestructive evaluation)*. Duluth (GA): Tech-Science Press, 1 ed., 2006.
[9] G. Aubert, J.-F. Jacquinot, and D. Sakellariou, "Eddy current effects in plain and hollow cylinders spinning inside homogeneous magnetic fields: application to magnetic resonance," *Journal of Chemical Physics*, vol. 137, no. 154201, pp. 1–14, 2012.
[10] P. R. Rony, "The electromagnetic levitation of metals," tech. rep., May 1964.
[11] G. Lohöfer, "Theory of an electromagnetically levitated metal sphere I: Absorbed power," *SIAM Journal of Applied Math*, vol. 49, no. 2, pp. 567–581, 1989.
[12] C. P. Bidinosti, E. M. Chapple, and M. E. Hayden, "The sphere in a uniform RF field—revisited," *Concepts in Magnetic Resonance Part B: Magnetic Resonance Engineering*, vol. 31B, no. 3, pp. 191–202, 2007.
[13] G. Sinha and S. S. Prabhu, "Analytical model for estimation of eddy current and power loss in conducting plate and its application," *Physical Review Special Topics-Accelerators and Beams*, vol. 14, no. 062401, pp. 1–10, 2011.
[14] R. F. Harrington, *Time-Harmonic Electromagnetic Fields*. 2 ed., 2001, publisher =.
[15] J. D. Jackson, *Classical Electrodynamics*. Hoboken (NJ): Wiley, 3 ed., 1999.
[16] Computer Simulation Technology, CST EM Studio, 2015. www.cst.com.
[17] O. Biro and K. Preis, "On the use of the magnetic vector potential in the finite element analysis of three-dimensional eddy currents," *IEEE Transactions on Magnetics*, vol. 25, no. 4, pp. 3145–3159, 1989.
[18] T. Strouboulis, I. Babuska, and R. Hidajat, "The generalized finite element method for Helmholtz equation: Theory, computation, and open problems," *Computational Methods in Applied Mechanical Engineering*, vol. 195, no. 37–40, pp. 4711–4731, 2006.
[19] Y. S. Wong and G. Li, "Exact finite difference schemes for solving Helmholtz equation at any wavenumber," *International Journal of Numerical Analysis and Modeling, Series B*, vol. 2, no. 1, pp. 91–108, 2011.
[20] G. B. Arfken and H. J. Weber, *Mathematical Methods for Physicists*. New York: Academic Press, 5 ed., 2001.